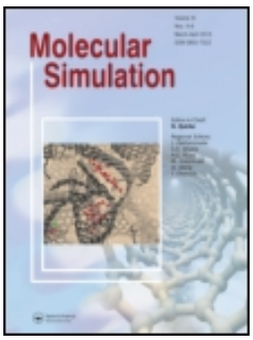

Molecular Simulation

ISSN: 0892-7022 (Print) 1029-0435 (Online) Journal homepage: http://www.tandfonline.com/loi/gmos20

Comprehensive genetic algorithm for ab initio global optimisation of clusters

Jijun Zhao, Ruili Shi, Linwei Sai, Xiaoming Huang & Yan Su

To cite this article: Jijun Zhao, Ruili Shi, Linwei Sai, Xiaoming Huang & Yan Su (2016) Comprehensive genetic algorithm for ab initio global optimisation of clusters, Molecular Simulation, 42:10, 809-819, DOI: 10.1080/08927022.2015.1121386

To link to this article: http://dx.doi.org/10.1080/08927022.2015.1121386

Published online: 04 Apr 2016.

MOLECULAR SIMULATION, 2016
VOL. 42, NO. 10, 809–819
http://dx.doi.org/10.1080/08927022.2015.1121386

Taylor & Francis
Taylor & Francis Group

SPECIAL ISSUE: FRONTIERS OF MOLECULAR SIMULATION IN CHINA

Comprehensive genetic algorithm for *ab initio* global optimisation of clusters

Jijun Zhao[a], Ruili Shi[a], Linwei Sai[b], Xiaoming Huang[c] and Yan Su[a]

[a]Key Laboratory of Materials Modification by Laser, Ion and Electron Beams, Dalian University of Technology, Dalian, P.R. China; [b]Department of Mathematics and Physics, Hohai University, Changzhou, P.R. China; [c]School of Ocean Science and Technology, Dalian University of Technology, Panjin, P.R. China

ABSTRACT

Cluster, as the aggregate of a few to thousands of atoms or molecules, bridges the microscopic world of atoms and molecules and the macroscopic world of condensed matters. The physical and chemical properties of a cluster are determined by its ground state structure, which is significantly different from its bulk structure and sensitively relies on the cluster size. As a well-known nondeterministic polynomial-time hard problem, determining the ground state structure of a cluster is a challenging task due to the extreme complexity of high-dimensional potential energy surface (PES). Genetic algorithm (GA) is an efficient global optimisation method to explore the PES of clusters. Recently, we have developed a GA-based programme, namely comprehensive genetic algorithm (CGA), and incorporated it with *ab initio* calculations. Using this programme, the lowest energy structures of a variety of elemental and compound clusters with different types of chemical bonding have been determined, and their physical properties have been investigated and compared with experimental data. In this article, we will describe the technique details of CGA programme and present an overview of its successful applications.

ARTICLE HISTORY
Received 2 October 2015
Accepted 12 November 2015

KEYWORDS
Cluster; global optimisation; genetic algorithm; structure

1. Introduction

Cluster, as the aggregate composed of a few to thousands of atoms or molecules, represents the intermediate state between microscopic atoms or molecules and macroscopic condensed matters.[1–7] Due to surface effect and quantum confinement effect, the physical and chemical properties of a cluster may differ from its bulk counterparts significantly. The exotic properties of clusters offer many opportunities to construct novel nanoscale materials and devices.

For a small- or medium-sized cluster with less than 300 atoms, more than half of the atoms locate on the surface. Adding one more atom to the cluster would lead to substantial structural reconstruction. As a consequence, the atomic structure of a cluster is usually rather different from a piece of the corresponding bulk solid. Indeed, one of the most fundamental and challenging problems in cluster science is to determine the ground state structure of a cluster. From the mathematic point of view, finding global minimum on the multidimensional potential energy surface (PES) of a cluster is a well-known nondeterministic polynomial-time hard problem.[8] As cluster size increases, the number of possible isomers on the PES may increase exponentially with the number of atoms.[9]

In experiments, clusters are usually generated in gas phase and detected via time of flight mass spectroscope and other spectroscopic means, e.g. photoelectron spectrum, infrared spectrum, electron diffraction, optical adsorption. However, direct determination of cluster structure by experiments alone is still rather difficult yet. Alternatively, by combining theoretical simulations and experimental measurements, a complete description of the atomic structure and physical properties of a cluster can be established.

Early theoretical efforts of determining the ground state structures of clusters usually involve the simulated annealing (SA) technique.[10] In the SA procedure, the system is first heated up to a high temperature (exceeding the melting point) and then gradually cooled down to room temperature via molecular dynamics (MD) or Monte Carlo simulations, which can be combined with either empirical potentials or first-principles methods. Even though SA procedure combined with first-principles calculations is a robust method and has been successfully employed to a series of clusters, such as Cd_nTe_n (n = 1–14),[11] Li_n (n = 20, 30, 40, 50),[12] P^+_{2m+1} (m = 1–12),[13] B_{28},[14] B_{80},[15] and $B_{101-103}$,[16] it cannot guarantee the global minimum of the PES unless the annealing time is sufficiently long.

Genetic algorithm (GA) is a widely used method to determine the global minimum structure of a system. Inspired by the Darwinian evolution theory that only the fittest candidates can survive, the basic philosophy of GA is to mimic the natural selection and evolution processes in nature.[17–19] The essential idea of GA is to allow a population of individual candidates to evolve under a given selection rule that maximises the fitness function. Compared to SA, GA can sample the PES more efficiently and hop from one region of the PES to another region rather easily.

CONTACT Jijun Zhao zhaojj@dlut.edu.cn; Linwei Sai sailinwei@hhu.edu.cn

The GA programme was first developed by Holland [18] and further generalised by Goldberg [19] in the fields of artificial intelligence and machine learning. Since 1993, there have been several pioneering works of utilising GA to determine the cluster structures, showing impressive efficiency.[20–37] An extraordinary example is the derivation of buckyball structure of C_{60} starting from a random configuration by Deaven and Ho.[23] Motivated by this success, there have been increasing interests in the applications of GA to search the global minima of a variety of clusters from noble gas clusters to metal and semiconductor clusters. In those early studies, the PESs of clusters were approximately described by semi-empirical models or empirical potentials,[27–37] and further first-principles calculations were performed to refine the candidate structures from empirical GA search. Although such hybrid strategy significantly reduces the computational cost with regard to full *ab initio* search, its reliability might be questionable, especially for those clusters with complicated bonding and cannot be well described by any empirical potentials.

In the past decade, benefitting from the rapid speeding-up of computer hardware, there has been significant progress in directly combining GA with *ab initio* methods to improve the accuracy and generality of GA-based global search. Independently, different groups in the world have developed their own GA codes for *ab initio* optimisation of clusters.[23,26,38–43] A large variety of elemental clusters have been explored, such as K_n ($n \le 20$),[44] Cs_n ($n \le 20$),[45] Al_n^+ and Al_n^- ($n \le 34$),[46] Cu_9,[47] Ga_n ($n \le 25$),[48] Pb_{4-15}^+ and Pb_{4-15}^-,[49] Bi_{4-14}^+,[50] P_{20} and As_{20}.[51] Furthermore, plenty of efforts using first-principles GA methodology have been devoted to alloy clusters, such as Si_4Li_{1-7},[52] Cu_nAg_{8-n} and Cu_nAu_{8-n},[53] $Au_{8-m}Ag_m$ ($1 < m < 8$),[54] $PtHf_{12}$ and $LaPb_7Bi_7$,[55] $Sn_{9-n}Bi_n$ ($n = 0$–4),[56] $Sn_{m-n}Bi_n$ ($m = 5$–13, $n = 1$–2),[57] as well as metal oxide clusters such as $(LiO)_{1-8}$,[58] $(BeO)_{2-24}$,[59] $(B_2O_3)_{1-6}$,[60] $(MgO)_{2-7}$,[61] $(TiO_2)_n$ with n up to 20,[62] $Ce_2O_2^+$, $Ce_3O_4^+$, $(CeO_2)_mCeO^+$ ($m = 0$–4),[63] and $(La_2O_3)_{1-6}$.[64] In addition, some molecular clusters or cluster complexes, such as $(H_2O)_3$ and $(ZnF_2)_{1-3}$,[52] $H(H_2O)_{1-4}$,[65] $(AlH_3)_{1-8}$,[66] $(LiF)_{1-30}F^-$,[67] CB_7^-,[68] $B_nAl_{6-n}^{2-}$ ($n = 0$–6),[69] $[Ag_7(SR)_4]^-$ and $[Ag_7(DMSA)_4]^-$,[70] and M_8 on TiO_2(110) surface with M = Ru, Rh, Pd, Ag, Pt, Au,[55] have also been investigated by GA-DFT approaches. Some of the progress has been reviewed by Heiles and Johnston.[41]

Recently, our group has developed a GA-based programme incorporated with *ab initio* calculations, namely comprehensive genetic algorithm (CGA). Using this approach, the lowest energy structures of a variety of clusters, such as closed-shell Na_n^+ ($n = 9$, 21, 41 and 59) and open-shell Na_n^+ ($n = 15$, 26, 31, 36 and 50),[71] Ca_{2-22},[72] Ga_{20-40} clusters,[73] Na_mSi_n ($1 \le m \le 3$, $1 \le n \le 11$) clusters,[38] Au_mAg_n with $5 \le m + n \le 12$,[74] Pt_nSn_n ($n = 1$–10) and $Pt_{3m}Sn_m$ ($m = 1$–5),[75] $V_3Si_{3-14}^-$,[76] $A@B_{12}@A_{20}$ (A = Sn, Pb; B = Mg, Zn, Cd, Mn) [77] and $(WO_3)_{2-12}$ clusters,[78] have been determined and their electronic properties have been investigated and compared with experiments. In the following, we will describe the technique details of CGA for cluster optimisation and give some examples for the practical applications of CGA for different kinds of elemental clusters, alloy clusters and metal oxide clusters. Finally, we give a brief summary and an outlook of the GA-based *ab initio* global optimisation methods.

2. Comprehensive genetic algorithm

When implemented into cluster research, GA is based on a population of individuals, each individual representing a cluster structure. The evolutionary principles are adopted to identify the optimal cluster structure.[26,39,40,79] Then genetic operations such as mating, mutation and natural selection are applied. The fittest members in the population survive and pass their genetic information to the subsequent generations (offspring) to produce descendants with improved quality.

As a typical GA procedure, the flow chart of our GGA programme for cluster optimisation is shown in Figure 1. Initially, the original population contains a number of cluster structures (N_p) generated in a random manner with some restriction rules (e.g. any of two atoms cannot stay too close; all atoms should be located within a given maximum radius). Usually, 16–64 clusters are generated to form an initial population. In principle, a larger population should be used if the cluster size is larger or the structure is very complicated. Practically, it is preferable to generate a much larger number of the initial members in the population and discard most of the high-energy (less-favourable) ones via natural selection.

After the structures of all initial candidates in the population are optimised by DFT calculations, the genetic operators are applied. The two major operators are mating (crossover) and mutation. One individual in the population is randomly selected as a father with a probability related to its total energies. Optionally, the roulette technique (a roulette wheel with slot widths corresponding to the fitness values of the cluster) is used and the structure with lower energy has more chance to be selected. Then a random number between zero to one is used to decide whether a mother is needed or not. If the random number is bigger than the mutation rate (usually choosing to be 0.1–0.3), a mating operation is employed; otherwise 'single-parent' mutation operation is selected.

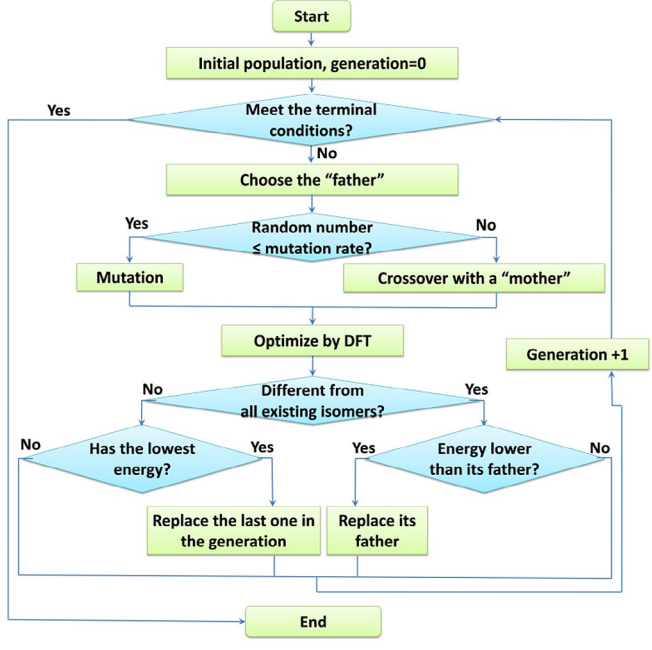

Figure 1. (colour online) Flow chart of comprehensive genetic algorithm incorporated with DFT calculations for cluster optimisation.

In the mating operation, we randomly choose another cluster from the population as a 'mother' to produce a child cluster via a 'cut and splice' crossover operation.[23] After being introduced for 20 years, this operation is shown to be efficient and robust, since one can combine the advantages of father and mother clusters. However, the conventionally used 'cut and splice' crossover method tend to reach sphere-like shape, which makes it unable to locate some non-spherical structures. For a non-spherical cluster with flat or strip-like shape, its father and mother may have two different directions and it is hard to combine them along the same direction to form a flat or strip-like structure. Based on this consideration, a new kind of crossover method, namely the 'principal direction cross', has been invented in our CGA programme to avoid the above-mentioned shortcoming. We first rotate the longest axis to x axis as the principal direction and the shortest axis to z axis; then we cut the structure along yz plane.

We set coordinate matrix A,

$$A = \begin{pmatrix} x_1 & y_1 & z_1 \\ x_2 & y_2 & z_2 \\ \vdots & \vdots & \vdots \\ x_n & y_n & z_n \end{pmatrix}$$

where (x_i, y_i, z_i) is the coordinates of the ith atom. We do singular value decompose for matrix A.

$$A = U\Sigma V^{\mathrm{T}}, \tag{1}$$

where U and V are orthogonal matrices and Σ is a diagonal matrix with diagonal elements as singular values in descending order. Let

$$B = AV^{\mathrm{T}}. \tag{2}$$

Then a new cluster with coordinate matrix B is generated by rotating cluster A.

As demonstrated by the core-orbits approach, the use of approximate symmetry substantially improves the efficiency of global optimisation for clusters.[80] Here we also introduce a method to search for symmetric clusters. For a given point group symmetry, we maintain all populations with this symmetry throughout all GA procedures, including generating the initial structures, crossover and mutation operations, and local DFT optimisations. We fix the symmetry axis to z-axis (for C_s symmetry, the symmetry plane is xy). Taking crossover operation as an example, before the cut operation, we first make a random rotation of a parent cluster in the 'cut and splice' method. Here we only perform rotation around the z-axis; then we cut along xy plane. Only four kinds of point group symmetries (C_s, C_2, C_3, C_5) are implemented in our CGA programme because these four symmetry groups are subgroups for most higher symmetry point groups.

In the above step of GA iteration, if the random number is smaller than the mutation rate, we adopt (single-parent) mutation operation, through which the child cluster directly inherits from its father with some structural modification. In practice, GA search may converge very rapidly to the minimum of a region of the configurational space, which is usually not the global minimum. Therefore, the advantage of mutation is to avoid being trapped in the local minima of PES. In CGA programme, we use the following mutation operations:

(1) Give every atom of a cluster a small random displacement less than 10% of the average bond length. This would help the cluster to find its local minimum on the PES nearby.
(2) Move a randomly chosen atom to the neighbouring location of another randomly chosen atom and avoid unreasonable overlap with any existing atom.
(3) For an alloy or compound cluster, exchange the atomic type of a pair of atoms. The influence of exchanging atomic type for minimising the total energy of a cluster could be tremendous.

After mating or mutation procedure, the offspring cluster is then relaxed using DFT optimisation. At each iteration of our CGA, DMol^3 [81,82] or the Vienna Ab initio Simulation Package (VASP) [83] is called to optimise the cluster structure and calculate the total energy. Usually, we choose intermediate convergence criteria for self-consistent field electronic structure calculation and geometry relaxation to maintain a balance between computational accuracy and efficiency.

To ensure the diversity of population, the 'selection' operation in the GA search is crucial. Several selection criteria are used:

(1) If the energy of a 'child' is higher than all existing 'parents', it should be thrown away.
(2) If the configuration of a 'child' is isomorphic to an existing individual in the population while its total energy is lower, it will enter the population and replace the existing isomorphic one.
(3) If the energy of a 'child' cluster is lower than some individuals in the population and its geometry is not identical to any of the existing ones, it will replace the 'worst' individual with highest total energy in the population.

We adopt the pseudo-rotational inertia of a cluster [38] defined by Equations (3) and (4) to identify whether two cluster geometries are isomorphic,

$$I = \sum_i m_i r_i^2 \tag{3}$$

$$I' = \sum_i m_i r_i^4 \tag{4}$$

where r_i is the distance of the ith atom from mass centre of cluster and m_i is the (fictitious) mass of the ith atom. In addition to the second-order inertia in Equation (3), Equation (4) defines a high-order inertia to judge the isomorphism of cluster geometries more accurately. In practice, two different structures may have close values of inertia I, but their I' values are likely to deviate from each other. For an elemental cluster, m of every atom is identical and set as 1. For an alloy cluster, $m = 1$ for one element a and $m = 2$ for another element b in Equation (3); inversely, $m = 2$ for element a and $m = 1$ for element b in Equation (4).

After the 'natural selection' procedure, the total number of individuals in the population remains N_p and GA iteration continues until the convergence is achieved or the maximum number of iterations (usually one to a few thousands) is reached.

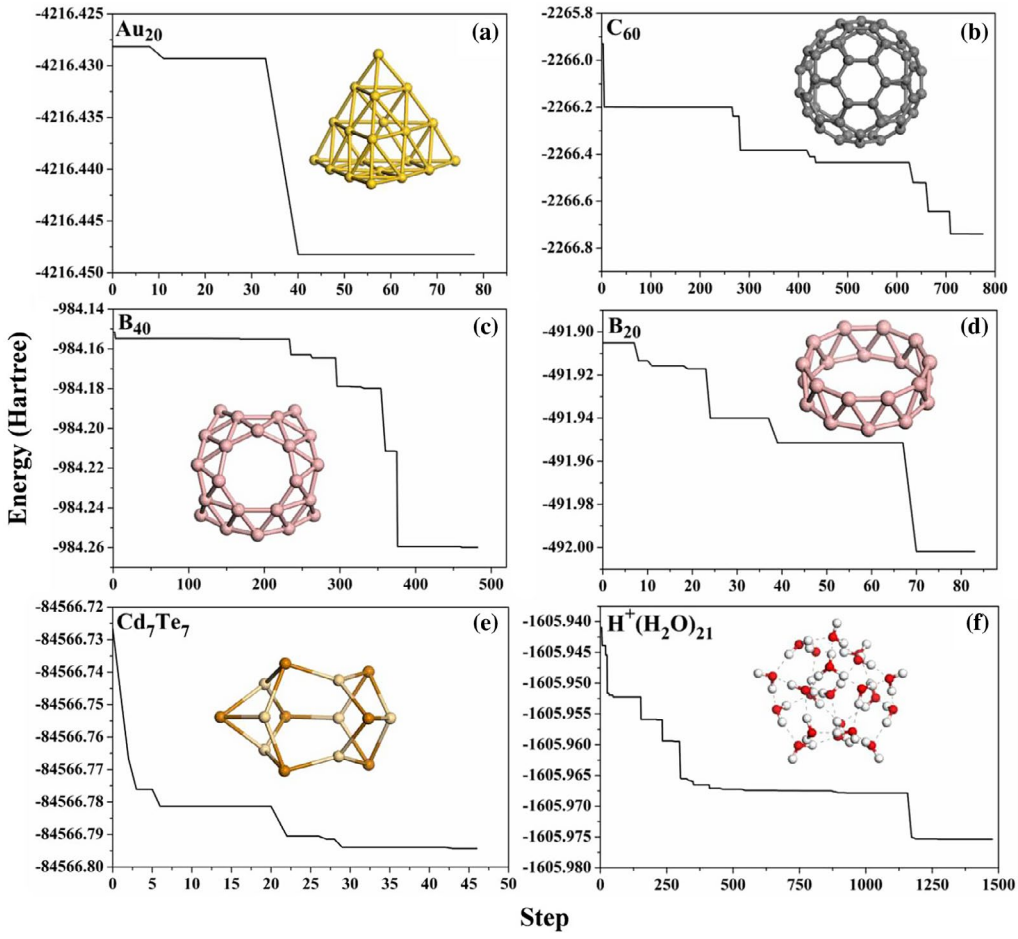

Figure 2. The energy evolutions with the GA iterations for six representative clusters searched using our CGA-DFT method. The final lowest energy structures are given in the insets. The symmetries of lowest-energy structures of Au_{20}, C_{60}, B_{40}, B_{20} and Cd_7Te_7 are T_d, I_h, D_{2d}, D_{10d} and C_{3v}, respectively.

In principle, all kinds of GA methods are similar, with slight difference in the technique details.[23,40,41]

3. Tests of CGA

To test the reliability of our CGA combined with *ab initio* calculation in DMol³ package, we study several representative atomic and molecular clusters, including Au_{20}, C_{60}, B_{20}, B_{40}, Cd_7Te_7 and $H^+(H_2O)_{21}$. Figure 2 shows the evolutions of cluster total energy with the GA iteration for the six clusters.

Gold is a typical heavy element with pronounced relativistic effect, and gold nanoclusters exhibit unusual catalytic capabilities. Au_{20} is a magic number cluster with a surprisingly tetrahedron configuration.[84,85] Due to the T_d symmetry as well as close-shell electronic structure, Au_{20} manifests enhanced stability. Using CGA-DFT method with C_3 symmetry restriction, we are able to reach the tetrahedron structure of Au_{20} within 40 GA generations (Figure 2(a)). Without presumed symmetry, about 1800 GA iterations are needed to obtain the Au_{20} tetrahedron. For comparison, Aprà et al. used basin hopping (BH) algorithm [86] combined with DFT to search the PES of Au_{20} cluster.[84] Three independent BH searches were performed and T_d configuration was obtained after 233, 28 and 177 steps, respectively.

Compared to metal clusters, semiconductor clusters may exhibit more complicated PESs due to the intrinsic nature of covalent bonding. Here we choose the famous C_{60} fullerene as an example, which was discovered by Kroto and co-workers in 1985 [87] and attracted significant attentions thereafter. In our CGA global search of C_{60}, we set C_3 symmetry and locate the buckyball structure in about 700 steps (see Figure 2(b)). Note that the pioneering study by Deaven and Ho [23] used about 6000 GA iterations to obtain the buckyball, since that the PES of C_{60} is very complicated with many barriers. The success for C_{60} using our programme taking the advantage of symmetry confirms its high efficiency for large semiconducting clusters with covalent bonding.

Stimulated by discovery of C_{60} fullerene, many efforts have been attempted to explore the possible all-boron fullerene.[14,88–91] Recently, Zhai et al. conducted a combined experimental and theoretical exploration of all-boron fullerene B_{40} and B_{40}^-.[91] For neutral B_{40} cluster, they performed an unbiased global search by using the stochastic surface walking [92] and BH algorithms, and confirmed that the fullerene-like cage with D_{2d} symmetry is the most stable structure of B_{40}. Using our CGA programme with C_2 symmetry, we obtain the lowest energy D_{2d} cage structure of B_{40} in 500 steps, as shown in Figure 2(c). On the other hand, our global search is able to reproduce the double-ring tubular structure of B_{20}

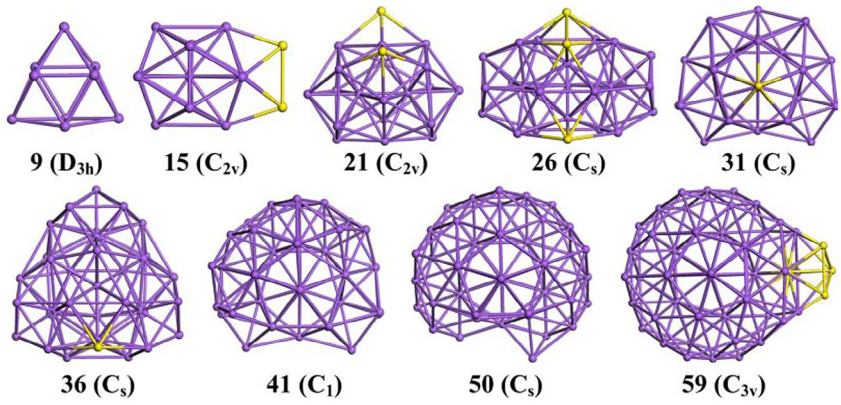

Figure 3. Lowest energy structures of Na_n^+ clusters (n = 9, 15, 21, 26, 31, 36, 41, 50 and 59). The symmetry for each cluster is given in the parenthesis. The additional atoms not belonging to the major building units of icosahedron or double icosahedron are highlighted in yellow (light) for the guide of the eyes. Reproduced with permission from Ref. [71]. © (2013) Springer-Verlag GmbH.

within 70 GA generations (see Figure 2(d)), which was previously reported by Kiran et al. using more than 1000 steps of BH search.[93] This result demonstrates that our CGA programme is also rather efficient for locating the oblate cluster structures.

In addition to the elemental clusters with metallic or covalent bonding, we also considered typical II–VI compound clusters with technological importance, i.e. Cd_nTe_n cluster. Previously, our group performed an unbiased SA search using *ab initio* MD and showed that three-dimensional (3D) cage structures of Cd_nTe_n clusters occur at n = 6.[11] Here we choose binary Cd_7Te_7 cluster as a testing model. Figure 2(e) shows the evolution of CGA search of Cd_7Te_7 and its global minimum configuration. From the initial random structure, the energy of cluster drops rapidly in the first five GA steps. Finally, the global minimum of Cd_7Te_7 cluster with three six-membered rings and six four-membered rings emerges in less than 50 steps, showing that CGA is capable of dealing with compound clusters.

Compared to the atomic clusters discussed above, global optimisation of molecular clusters is even more challenging since it evolves translation and rotation of 'quasi-rigid' molecules and accurate description of non-covalent intermolecular interaction. Protonated water clusters widely exist in aqueous solution and play an important role in many chemical and biological reactions. Among them, $H^+(H_2O)_{21}$ is a magic number cluster, as identified by Lin using a quadrupole mass filter.[94] Several successive studies revealed that the lowest energy structure of $H^+(H_2O)_{21}$ is a distorted pentagonal dodecahedral (5^{12}) cage with a H_2O molecule in the centre and a H_3O^+ ion on the surface, which has nine dangling OH bonds on the surface. [95–98] Figure 2(f) shows the evolution for structure prediction of $H^+(H_2O)_{21}$ cluster using CGA. With a population of 16 candidates, CGA search takes about 1200 iterations to locate this global minimum configuration without any symmetry setting. This success further proves that our CGA programme is also applicable to molecular clusters.

4. Applications of CGA

4.1. Elemental clusters

As predicted by the shell model,[1] a simple metal cluster with closed electronic shell should possess 8, 20, 40, 58 … valence electrons. To explore the interplay between atomic and electronic structures, the closed-shells Na_n^+ clusters with n = 9, 21, 41 and 59 as well as several open-shell Na_n^+ clusters with n = 15, 26, 31, 36 and 50 were studied by our group using CGA-DFT.[71] The lowest energy structures of these Na_n^+ clusters are shown in Figure 3, and the photoabsorption spectra of selected Na_n^+ clusters from time-dependent DFT (TD-DFT) [99] simulations are compared to the experimental ones in Figure 4. The excellent agreement between theory and experiment confirms the reliability of our theoretical appro aches.

As displayed in Figure 3, the Na_n^+ clusters generally adopt icosahedron-based compact structures. For the small clusters, Na_9^+ has a tricapped trigonal prism configuration with D_{3h} symmetry; then Na_{15}^+ can be obtained by adding two sodium atoms on the nearby facets of a 13-atom icosahedron. The most stable structure of Na_{21}^+ cluster can be regarded as a double icosahedron of Na_{19} with two additional Na atoms capped on the waist. Na_{26}^+ is composed of two icosahedra sharing three Na atoms on the middle triangle face with remaining three Na atoms located on the middle region. A T_d symmetry structure formed

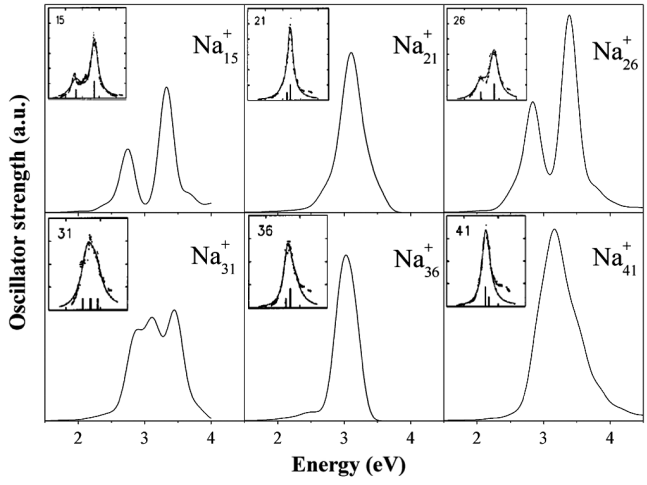

Figure 4. Photoabsorption spectra of the Na_n^+ clusters (n = 15, 21, 26, 31, 36, 41) from TD-DFT simulations. The corresponding experimental data are shown in insets. Reproduced with permission from Ref. [71]. © (2013) Springer-Verlag GmbH.

by four interpenetrating icosahedra from empirical simulation with Gupta and MM potentials of Na_{26} [100] is less stable by 0.058 eV. The ground state configuration of Na_{31}^+ consists of two interpenetrating double icosahedra with one additional Na atom capped on the middle. The most favourable geometry of Na_{36}^+ can be achieved by adding one atom on a C_{3v} symmetric structure of Na_{35}.[101] It prevails the spherical disordered structures with high compactness predicted from empirical Gupta and MM potentials by 0.24 and 0.30 eV, respectively.[100] Interestingly, the lowest energy structure of Na_{41}^+ with closed electronic shell (40 valence electrons) deviates significantly from a perfect sphere as predicted by jellium model, but is a hemisphere by removing some atoms from a 55-atom Mackay icosahedron. This indicates that geometry effect plays a remarkable role. According to our DFT calculations, the energy of present Na_{41}^+ structure is 0.05 eV lower than that from Gupta potential and 0.09 eV lower than that from the MM potential,[100] respectively. The ground state structure of Na_{50}^+ follows the Mackay icosahedral motif and is an incomplete icosahedron with lack of five Na atoms. Na_{59}^+ is also based on the Mackay icosahedron of Na_{55} with a four-atom tetrahedron added on a triangle face. Overall speaking, the ground-state structures of Na_n^+ clusters obtained by CGA-DFT search are lower in energy than most of previously reported ones with empirical potentials.

As another example of metal clusters, Liang et al. have performed DFT-based GA search for the ground state configurations of neutral and anionic Ca_n clusters with n = 2–22.[72] Except for n = 13–17, neutral and anionic Ca_n clusters share the same ground state structures, as shown in Figure 5. For Ca_n clusters with $n \geq 11$, the most stable configurations adopt pentagonal bipyramid or hexagonal pyramid as the main skeleton. The vertical detachment energies (VDEs) and adiabatic detachment energies (ADEs) of anionic Ca_n clusters from DFT calculations also compare well with the experimental data,[102] confirming the validity of the theoretical results.

Gallium is a trivalent metal element with unusual structural and bonding characteristics, whose solid state is known to exhibit at least nine polymorphs. As the embryo of bulk solid, gallium clusters have also received considerable attentions. Sai et al. carried out an unbiased GA search combined with DFT to determine the most stable structures of medium-sized Ga_n clusters (n = 20–40).[73] Compared to the other metal clusters, the structures of medium-sized gallium clusters are more complicated and less compact. Except for Ga_{23} (D_{3h}), Ga_{25} (D_{3h}) and Ga_{36} (D_{2d}), most Ga_n clusters exhibit no symmetry or low symmetry. Starting from Ga_{31}, core-shell structures with four to six interior atoms become the dominant structural motif. Among all Ga_n clusters studied, Ga_{36} stands out as a magic cluster with high symmetry, large binding energy and sizeable HOMO–LUMO gap, which can be partially related to the electron shell. For the rest of clusters between Ga_{32} and Ga_{39}, their structures can be all related to Ga_{36} by removing or moving atoms.

4.2. Alloy clusters

Besides elemental clusters, our CGA programme has also been successfully employed to study various alloy clusters. As the first assessment of CGA-DFT programme, the lowest energy configurations of neutral and ionic clusters of Na_mSi_n ($1 \leq m \leq 3$, $1 \leq n \leq 11$) clusters have been systematically investigated by Sai et al. [38] As representatives, the ground state configurations of Na_3Si_n ($1 \leq n \leq 11$) clusters are shown in Figure 6. In neutral Na–Si clusters, Na atoms are usually separated from each other by the Si skeleton; while in anionic clusters, Na atoms stay together to form Na–Na bonds. For small clusters, the cluster structures are sensitive to both Na/Si stoichiometry and charge state; while for larger Na_nSi_m clusters with $m > 7$, addition of one Na atom or one extra charge would not result in significant change in the ground state structure. The experimental size dependences of ionisation potentials and electron affinities, as well as the photoelectron spectra of selected $Na_nSi_m^-$ clusters are satisfactorily reproduced

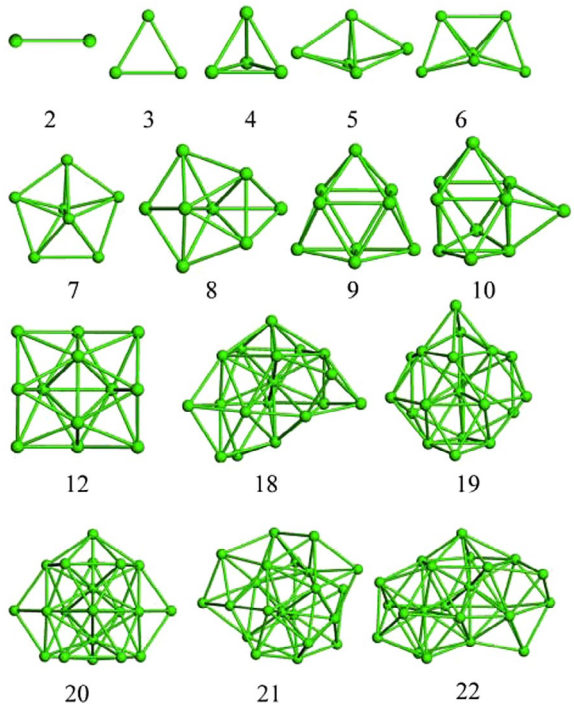

Figure 5. Ground state structures of neutral and anionic Ca_n clusters with n = 2–10, 12, 18–22. Reproduced with permission from Ref. [72]. © (2015) Elsevier Ltd.

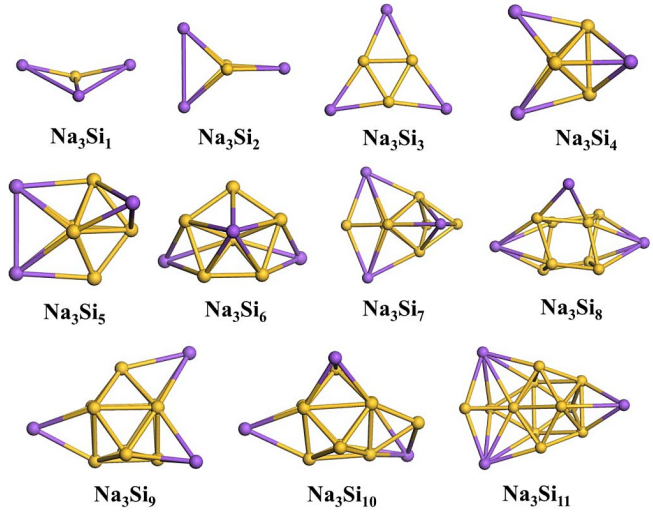

Figure 6. The lowest energy structures of Na_3Si_n ($1 \leq n \leq 11$) clusters from CGA-DFT search. Colour code: blue for Na, yellow for Si. Reproduced with permission from Ref. [38]. © (2011) American Institute of Physics.

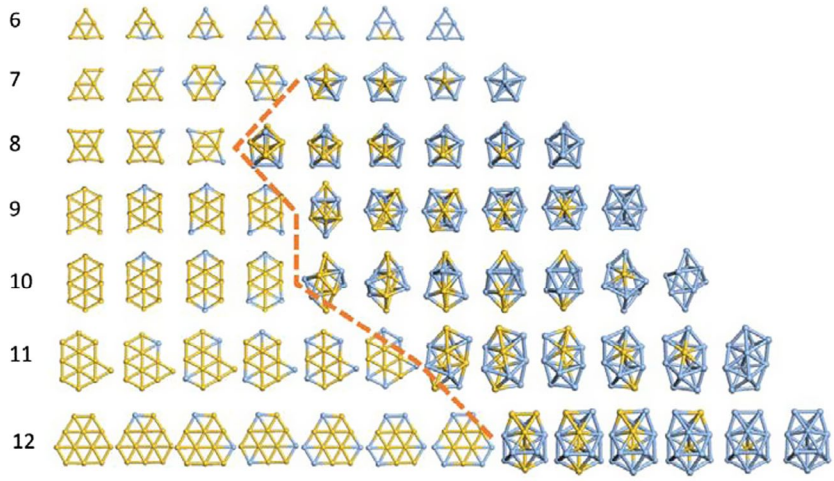

Figure 7. The lowest energy structures and some metastable isomers of Au_mAg_n ($6 \le m + n \le 12$) clusters. Left side: Au; right side: Ag. A split line divides the 2D and 3D structures of the Au–Ag clusters.

by theoretical calculations, confirming the reliability of our CGA-DFT approach.

Even belonging to the same group in the periodic table, small Ag_n clusters prefer 3D structures, while small Au_n clusters tend to adopt two-dimensional (2D) configurations due to the s–d hybridisation and the relativistic effects. Thus, binary Au–Ag clusters provide an ideal playground for exploring the competition between 3D and 2D structural motifs and the composition effect on alloy clusters. Using CGA-DFT method, atomic structures and energies of Au–Ag binary clusters are systematically studied by our group.[74] As illustrated in Figure 7, a split line divides the 2D and 3D structures of the Au–Ag clusters with totally 6–12 atoms. At each size, the 2D structures of Au–Ag alloy clusters usually share the same skeleton of pure Au clusters, while the 3D structures of binary clusters adopt the skeleton same as pure Ag clusters. For the binary clusters with 7, 11 and 12 atoms, the Au:Ag ratio for 2D–3D transition is close to 1, suggesting that the influences of Au and Ag atoms are comparable. As for the binary systems with 8, 9 and 10 atoms, the 2D–3D transition occurs at Au_5Ag_3, Au_5Ag_4 and Au_6Ag_4, respectively. In an independent GA-DFT study, Johnston et al. [54] investigated the 8-atom Au–Ag alloy clusters and also found a transition from 2D to 3D structure between Au_6Ag_2 and Au_5Ag_3 consistent with our result.

Recently, our CGA-DFT approach has been used to investigated the low-energy structures of Pt_nSn_n ($n = 1$–10) and $Pt_{3m}Sn_m$ ($m = 1$–5) clusters, which can be considered as nanoscale model catalysts.[75] In general, Pt and Sn prefer to mix with each other and Sn atoms on the surface tend to segregate due to the energetically favourable Pt–Sn bonds as well as the larger atomic radii of Sn atoms. This makes one or two Pt atoms available for reaction. With more than four atoms, 3D cluster structures emerge. Pt_2Sn_2 quadrilaterals as basic structural units of PtSn solid can be found in many cluster isomers. For $Pt_{3m}Sn_m$ clusters with larger ratio of Pt atoms, Sn atoms are well separated without forming any Sn–Sn bond. As the cluster grows bigger, there is a distinct tendency of layered structures consisting of Pt–Sn alternative triangular lattices, resembling Pt_3Sn solid.

The elemental silicon clusters have surface dangling bonds, which renders them chemically reactive and therefore not suitable for building blocks of nanoscale materials and devices. It has been shown both theoretically and experimentally that incorporation of transition metal (TM) atoms into a silicon cluster not only stabilises the cluster, but also brings in peculiar properties. So far, little is known about doping of multiple TM atoms inside Si clusters. Huang et al. [76] systematically studied $V_3Si_n^-$ (n = 3–14) clusters using CGA-DFT method and simulated the anion photoelectron spectra, VDEs and ADEs. The lowest energy structures and ADEs of $V_3Si_{3-14}^-$ from theoretical calculations are displayed in Figure 8, showing excellent agreement with experiment. In most $V_3Si_n^-$ clusters, three V atoms prefer to stay close with each other and form strong V–V bonds.

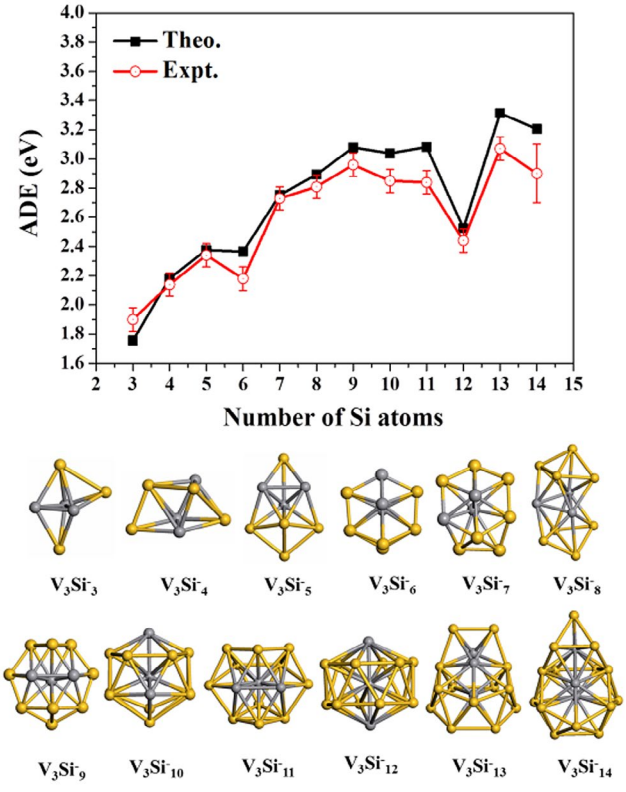

Figure 8. Adiabatic detachment energies (ADEs) (upper panel) and lowest energy structures of $V_3Si_n^-$ (n = 3–14) clusters. Reproduced with permission from Ref. [102]. © (2015) American Chemical Society.

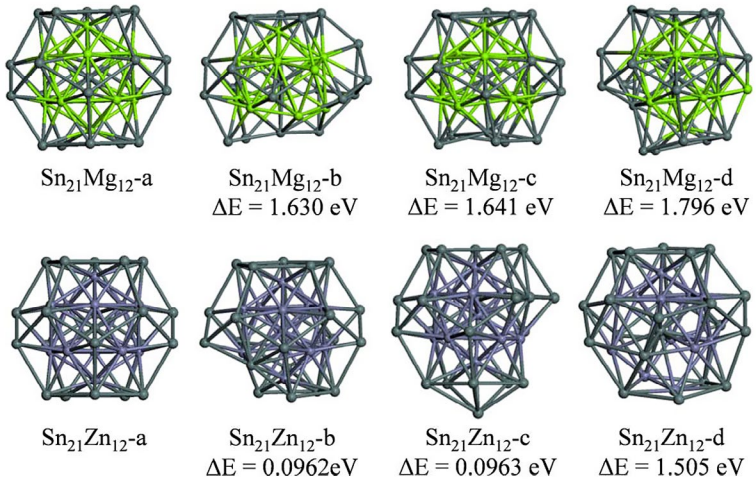

Figure 9. Low-lying isomer structures of $Sn@Mg_{12}@Sn_{20}$ and $Sn@Zn_{12}@Sn_{20}$ clusters. For each isomer, its energy difference to the ground state (denoted as a) is provided. Colour code: dark gray for Sn, green for Mg, light purple for Zn. Reproduced with permission from Ref. [77]. © (2014) Nature Publishing Group.

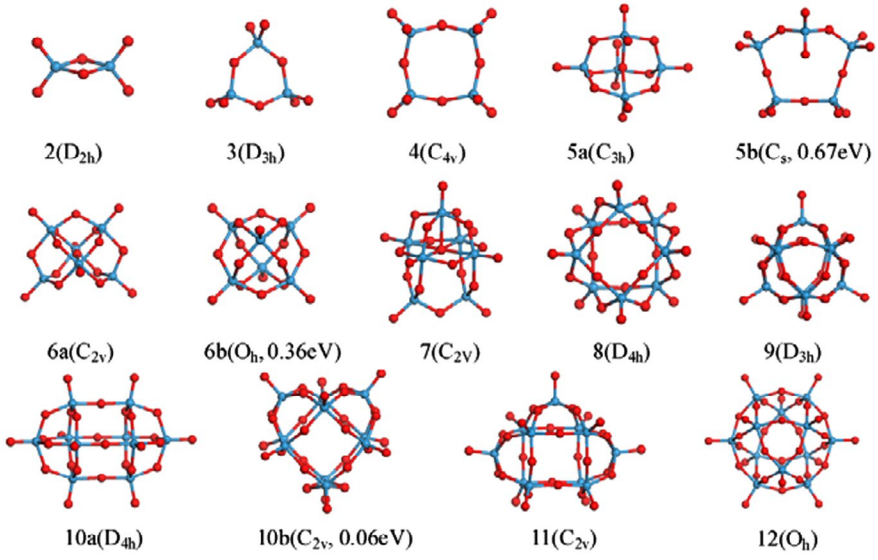

Figure 10. Lowest energy structures of $(WO_3)_n$ clusters ($2 \le n \le 12$) and selected metastable isomers (labelled as 5b, 6b, 10b). Reproduced with permission from Ref. [78]. © (2012) Elsevier Ltd.

Cage configurations with one interior V atom emerge for $V_3Si_n^-$ ($n \ge 11$). Most interestingly, V_3Si_{12} with D_{6d} symmetry carries a magnetic moment of 4 μ_B and the alignment of on-site magnetic moments exhibits ferrimagnetic ordering, i.e. +2.4 μ_B and −0.6 μ_B on the surface and the central V atoms, respectively.[103] The atomic structures and electronic properties from theoretical calculations can be further confirmed by the experimental photoelectron spectra of anionic $V_3Si_n^-$ (n = 3–14) and $V_mSi_{12}^-$ (m = 1–3) clusters.[103]

The existence of a kind of fascinating structures, i.e. onion-like icosahedral 'matryoshka' cluster, can be also confirmed by our CGA-DFT calculations.[77] This kind of 33-atom clusters with formula of $A@B_{12}@A_{20}$ (A = Sn, Pb; B = Mg, Zn, Cd, Mn) can be separated into three atomic shells. From global search using CGA-DFT, two representative clusters, i.e. $Sn_{21}Mg_{12}$ and $Sn_{21}Zn_{12}$, have been confirmed to adopt onion-like icosahedral 'matryoshka' structure as their ground state (see Figure 9). The high stability of these 'matryoshka' clusters is then attributed to suitable matching of atomic sizes as well as the high I_h symmetry and consequently the splitting of superatom orbitals of high angular momentum. Furthermore, two magnetic 'matryoshka' clusters, i.e. $Sn@Mn_{12}@Sn_{20}$ and $Pb@Mn_{12}@Pb_{20}$, are proposed by replacing fully filled d^{10} shell by half-filled d^5 shell. These magnetic superatoms possess a large magnetic moment of 28 μ_B, a moderate HOMO–LUMO gap, and weak inter-cluster interaction energy, making them ideal building blocks in novel magnetic materials and devices.

4.3. Metal oxide clusters

Apart from alloy clusters, metallic oxide clusters have also been studied by CGA-DFT. Using CGA-DFT approach, the lowest energy structures of $(WO_3)_n$ ($2 \le n \le 12$) clusters have been determined by Sai et al. [78], as displayed in Figure 10. It is found that small $(WO_3)_n$ clusters with n = 3, 4 adopt ring-like configurations with W–O alternating arrangement. Starting from $(WO_3)_8$, the

tungsten oxide clusters transform to symmetric spherical-like cages. Analysis of wavefunctions of frontier orbitals and electron density of states shows that the valence bands are dominated by the 2p electrons from O and the conduction bands are mainly contributed by the 5d states from W.

5. Summary and outlook

In this review, we present an overview of the CGA developed by our group, including its basic philosophy, technique implementation to clusters, results of test calculations and applications on various clusters.

As a widely used global minimisation method, the essential idea of GA is to inherit the merits of parent clusters via crossover operation and to avoid being trapped in local minimum via appropriate mutation on geometry. Incorporation of DFT calculations as local minimisation approach of the offspring clusters allows rather accurate description of the cluster PES, especially for those clusters with complicated bonding that cannot by described by empirical potential. As a result, our CGA-DFT strategy shows remarkable performance in locating the ground state structures of various clusters with different types of chemical bonds, from metallic to ionic and covalent, and to hydrogen bonding.

Despite the great success achieved by our CGA programme, it still has some limitations for wide applications on various clusters. One of the most critical concerns is the low efficiency for the long-term GA search. Usually, after the first 1000 or 500 iterations, it would be rather difficult to discover new lower energy structure, although the true global minimum might have not been located. Fortunately, there are still some rooms to improve the efficiency and robustness of CGA programme. It is tempting to utilize some bonding rules in compound clusters to create more reasonable initial configurations and to improve the crossover operation. Some new techniques are also needed in the implementation of GA on molecular clusters, e.g. how to effectively optimise the number and orientation of hydrogen bonds? It would be desirable to let GA learn the merits of other global optimisation algorithms such as BH, minima hopping, particle swarm optimisation, parallel temperature method, which may help improve the long-term searching efficiency. Further development of CGA programme along this direction is still under way and will be reported elsewhere.

As a tradeoff of high accuracy, application of the CGA-DFT method is also limited by its substantial computational costs. Within the current capability of standard computer power, the upper limit of cluster size explored by CGA-DFT is about 50–100 atoms, depending on the type of chemical bonding and consequently the complexity of the PES. To extend the scope of cluster size, it would be desirable to combine CGA (or other kind of GA) with some faster but still reasonably accurate DFT programme, other than the currently used VASP or DMol[3]. On the other hand, one has to be very cautious when dealing with some TM clusters, metal oxide clusters, molecular clusters and so on, since conventional DFT methods might not be accurate enough and fail in distinguishing the structural isomers for some particular systems. Sometimes, test calculations of the performance of DFT methods using more accurate *ab initio* method as benchmark are necessary.

Last but not least, the scope of GA method could be further extended to other related systems, e.g. clusters supported on substrate, ligand-protected metal clusters, one-dimensional nanowires and so on. By further developments of the algorithm itself along with the continuous increasing computer speed, we expect our CGA-DFT method would become a standard tool in cluster science and be used by many other groups in this field.

Disclosure statement

No potential conflict of interest was reported by the authors.

Funding

This work was supported by the National Natural Science Foundation of China [grant numbers 11134005, 11174045, 11574040, 11304030]; The Fundamental Research Funds for the Central Universities [grant number B2X/14B101-13].

References

[1] de Heer WA. The physics of simple metal clusters: experimental aspects and simple models. Rev. Mod. Phys. 1993;65:611–676. doi:10.1103/RevModPhys.65.611.
[2] Berry R, Haberland H. Clusters of atoms and molecules. Berlin: Springer; 1994. p. 1–12.
[3] Alonso JA. Electronic and atomic structure, and magnetism of transition-metal clusters. Chem. Rev. 2000;100:637–678. doi:10.1021/cr980391o.
[4] Baletto F, Ferrando R. Structural properties of nanoclusters: energetic, thermodynamic, and kinetic effects. Rev. Mod. Phys. 2005;77:371–423. doi:10.1103/RevModPhys.77.371.
[5] Ferrando R, Jellinek J, Johnston RL. Nanoalloys: from theory to applications of alloy clusters and nanoparticles. Chem. Rev. 2008;108:845–910. doi:10.1021/cr040090 g.
[6] Jena P, Castleman Jr AW. Nanoclusters: a bridge across disciplines. Vol. 1, Elsevier; 2010.
[7] Zhao J, Huang X, Jin P, et al. Magnetic properties of atomic clusters and endohedral metallofullerenes. Coord. Chem. Rev. 2015;289–290:315–340. doi:10.1016/j.ccr.2014.12.013.
[8] Wille LT, Vennik J. Computational complexity of the ground-state determination of atomic clusters. J. Phys. A. 1985;18:L419–L422. doi:10.1088/0305-4470/18/8/003.
[9] Hoare M. Structure and dynamics of simple microclusters. Adv. Chem. Phys. 1979;40:49–135.
[10] Kirkpatrick S, Gelatt CD, Vecchi MP. Optimization by simulated annealing. Science. 1983;220:671–680.
[11] Wang J, Ma L, Zhao J, et al. Structural growth behavior and polarizability of Cd_nTe_n (n = 1–14) clusters. J. Chem. Phys. 2009;130:214307-1–214307-8. doi:10.1063/1.3147519.
[12] Guo Z, Lu B, Jiang X, et al. Structural, electronic, and optical properties of medium-sized Li_n clusters (n = 20, 30, 40, 50) by density functional theory. Physica. E. 2010;42:1755–1762. doi:10.1016/j.physe.2010.01.039.
[13] Xue T, Luo J, Shen S, et al. Lowest-energy structures of cationic (m = 1–12) clusters from first-principles simulated annealing. Chem. Phys. Lett. 2010;485:26–30. doi:10.1016/j.cplett.2009.12.019.
[14] Zhao J, Huang X, Shi R, et al. B_{28}: the smallest all-boron cage from an *ab initio* global search. Nanoscale. 2015;7:15086–15090. doi:10.1039/C5NR04034E.
[15] Zhao J, Wang L, Li F, et al. B_{80} and other medium-sized boron clusters: core–shell structures, not hollow cages. J. Phys. Chem. A. 2010;114:9969–9972. doi:10.1021/jp1018873.
[16] Li F, Jin P, Jiang D-E, et al. B_{80} and $B_{101-103}$ clusters: remarkable stability of the core-shell structures established by validated density functionals. J. Chem. Phys. 2012;136:074302-1–074302-8. doi:10.1063/1.3682776.
[17] Davis L. Genetic algorithm and simulated annealing. Altos, CA United States: Morgan Kaufman Publishers, Inc.,Los; 1987.

[18] Holland JH. Adaption in Natural and Artificial Systems; Ann Arbor, MI: University of Michigan Press; 1978.

[19] Goldberg DE. Genetic algorithms in search, optimization and machine learning. New York: Addison-Wesley Longman Publishing; 1989.

[20] Hartke B. Global geometry optimization of clusters using genetic algorithms. J. Phys. Chem. 1993;97:9973–9976. doi:10.1021/j100141a013.

[21] Xiao Y, Williams DE. Genetic algorithm: a new approach to the prediction of the structure of molecular clusters. Chem. Phys. Lett. 1993;215:17–24. doi:10.1016/0009-2614(93)89256-H.

[22] Cartwright HM. Applications of artificial intelligence in chemistry. Oxford: Oxford University Press; 1993.

[23] Deaven DM, Ho KM. Molecular geometry optimization with a genetic algorithm. Phys. Rev. Lett. 1995;75:288–291. doi:10.1103/PhysRevLett.75.288.

[24] Hartke B. Global geometry optimization of clusters using a growth strategy optimized by a genetic algorithm. Chem. Phys. Lett. 1995;240:560–565. doi:10.1016/0009-2614(95)00587-T.

[25] Zeiri Y. Prediction of the lowest energy structure of clusters using a genetic algorithm. Phys. Rev. E. 1995;51:R2769–R2772. doi:10.1103/PhysRevE.51.R2769.

[26] Zhao J, Xie RH. Genetic algorithms for the geometry optimization of atomic and molecular clusters. J. Comput. Theor. Nanosci. 2004;1:117–131. doi:10.1166/jctn.2004.010.

[27] Wang J, Wang G, Zhao J. Structure and electronic properties of Ge_n (n = 2–25) clusters from density-functional theory. Phys. Rev. B. 2001;64:205411-1–205411-5. doi:10.1103/PhysRevB.64.205411.

[28] Wang J, Wang G, Zhao J. Density functional study of beryllium clusters, with gradient correction. J. Phys.: Condens. Matter. 2001;13:L753–L758. doi:10.1088/0953-8984/13/33/101.

[29] Zhao J, Luo Y, Wang G. Tight-binding study of structural and electronic properties of silver clusters. Eur. Phys. J. D. 2001;14:309–316. doi:10.1007/s100530170197.

[30] Zhao J. Density-functional study of structures and electronic properties of Cd clusters. Phys. Rev. A. 2001;64:043204-1–043204-5. doi:10.1103/PhysRevA.64.043204.

[31] Wang J, Wang G, Zhao J. Density-functional study of Au_n (n = 2–20) clusters: Lowest-energy structures and electronic properties. Phys. Rev. B. 2002;66:035418-1–035418-6. doi:10.1103/PhysRevB.66.035418.

[32] Wang J, Wang G, Zhao J. Nonmetal-metal transition in Zn_n (n=2–20) clusters. Phys. Rev. A. 2003;68:013201-1–013201-6. doi:10.1103/PhysRevA.68.013201.

[33] Yoo S, Zhao J, Wang J, et al. Endohedral silicon fullerenes Si_N ($27 \le N \le 39$). J. Am. Chem. Soc. 2004;126:13845–13849. doi:10.1021/ja046861f.

[34] Wang B, Zhao J, Chen X, et al. Atomic structures and covalent-to-metallic transition of lead clusters Pb_n (n = 2 – 22). Phys. Rev. A. 2005;71:033201-1–033201-7. doi:10.1103/PhysRevA.71.033201.

[35] Zhou X, Zhao J, Chen X, et al. Structural and electronic properties of Sb_n (n = 2 – 10) clusters using density-functional theory. Phys. Rev. A. 2005;72:053203-1–053203-6. doi:10.1103/PhysRevA.72.053203.

[36] Zhao J, Wang J, Jellinek J, et al. Stuffed fullerene structures for medium-sized silicon clusters. Eur. Phys. J. D. 2005;34:35–37. doi:10.1140/epjd/e2005-00113-x.

[37] Zhao J, Zhou X, Chen X, et al. Density-functional study of small and medium-sized Asn clusters up to n = 28. Phys. Rev. B. 2006;73:115418-1–115418-10. doi:10.1103/PhysRevB.73.115418.

[38] Sai L, Tang L, Zhao J, et al. Lowest-energy structures and electronic properties of Na-Si binary clusters from *ab initio* global search. J. Chem. Phys. 2011;135:184305–184309. doi:10.1063/1.3660354.

[39] Alexandrova AN, Boldyrev AI, Fu YJ, et al. Structure of the $Na_xCl_{x+1}^-$ (x = 1–4) clusters via *ab initio* genetic algorithm and photoelectron spectroscopy. J. Chem. Phys. 2004;121:5709–5719. doi:10.1063/1.1783276.

[40] Johnston RL. Evolving better nanoparticles: genetic algorithms for optimising cluster geometries. Dalton Trans. 2003;22:4193–4207. doi:10.1039/b305686d.

[41] Heiles S, Johnston RL. Global optimization of clusters using electronic structure methods. Int. J. Quantum Chem. 2013;113:2091–2109. doi:10.1002/qua.24462.

[42] Wu S, Ji M, Wang C-Z, et al. An adaptive genetic algorithm for crystal structure prediction. J. Phys.: Condens. Matter. 2014;26:035402-1–035402-6. doi:10.1088/0953-8984/26/3/035402.

[43] Sierka M. Synergy between theory and experiment in structure resolution of low-dimensional oxides. Prog. Surf. Sci. 2010;85:398–434. doi:10.1016/j.progsurf.2010.07.004.

[44] Abdalla S, Springborg M, Dong Y. Isolated and deposited potassium clusters: energetic and structural properties. Surf. Sci. 2013;608:255–264. doi:10.1016/j.susc.2012.10.016.

[45] Assadollahzadeh B, Thierfelder C, Schwerdtfeger P. From clusters to the solid state: global minimum structures for cesium clusters Cs_n (n = 2-20, ∞) and their electronic properties. Phys. Rev. B. 2008;78:245423-1–245423-11. doi:10.1103/PhysRevB.78.245423.

[46] Drebov N, Ahlrichs R. Structures of Al_n, its anions and cations up to n = 34: a theoretical investigation. J. Chem. Phys. 2010;132:164703-1–164703-7. doi:10.1063/1.3403692.

[47] Assadollahzadeh B, Bunker PR, Schwerdtfeger P. The low lying isomers of the copper nonamer cluster, Cu_9. Chem. Phys. Lett. 2008;451:262–269. doi:10.1016/j.cplett.2007.12.024.

[48] Drebov N, Weigend F, Ahlrichs R. Structures and properties of neutral gallium clusters: a theoretical investigation. J. Chem. Phys. 2011;135:044314-1–044314-7. doi:10.1063/1.3615501.

[49] Kelting R, Otterstätter R, Weis P, et al. Structures and energetics of small lead cluster ions. J. Chem. Phys. 2011;134:024311. doi:10.1063/1.3518040.

[50] Kelting R, Baldes A, Schwarz U, et al. Structures of small bismuth cluster cations. J. Chem. Phys. 2012;136:154309-1–154309-10. doi:10.1063/1.3703014.

[51] Nava P, Ahlrichs R. Theoretical investigation of clusters of phosphorus and arsenic: fascination and temptation of high symmetries. Chemistry. 2008;14:4039–4045. doi:10.1002/chem.200701927.

[52] Kanters RPF, Donald KJ. Cluster: searching for unique low energy minima of structures using a novel implementation of a genetic algorithm. J. Chem. Theo. Comp. 2014;10:5729–5737. doi:10.1021/ct500744k.

[53] Heard CJ, Johnston RL. A density functional global optimisation study of neutral 8-atom Cu-Ag and Cu-Au clusters. Eur. Phys. J. D. 2013;67:37–53. doi:10.1140/epjd/e2012-30601-7.

[54] Heiles S, Logsdail AJ, Schäfer R, et al. Dopant-induced 2D-3D transition in small Au-containing clusters: DFT-global optimisation of 8-atom Au-Ag nanoalloys. Nanoscale. 2012;4:1109–1115. doi:10.1039/C1NR11053E.

[55] Weigend F. Extending DFT-based genetic algorithms by atom-to-place re-assignment via perturbation theory: a systematic and unbiased approach to structures of mixed-metallic clusters. J. Chem. Phys. 2014;141:134103-1–134103-6. doi:10.1063/1.4896658.

[56] Heiles DIS, Hofmann K, Johnston PRL, et al. Nine-Atom Tin-Bismuth clusters: mimicking excess electrons by element substitution. Chem. Plus. Chem. 2012;77:532–535. doi:10.1002/cplu.201200085.

[57] Heiles S, Johnston RL. Bismuth-doped Tin clusters: experimental and theoretical studies of neutral Zintl analogues. J. Phys. Chem. A. 2012;116:7756–7764. doi:10.1021/jp304321u.

[58] Yuan Y, Cheng L. Theoretical prediction for the structures of gas phase lithium oxide clusters: $(Li_2O)_n$ (n = 1–8). Int. J. Quantum Chem. 2013;113:1264–1271. doi:10.1002/qua.24274.

[59] Ren L, Cheng L, Feng Y, et al. Geometric and electronic structures of $(BeO)_N$ (N = 2-12, 16, 20, and 24): rings, double rings, and cages. J. Chem. Phys. 2012;137:014309-1–014309-5. doi:10.1063/1.4731808.

[60] Li L, Cheng L. First principle structural determination of $(B_2O_3)_n$ (n = 1–6) clusters: from planar to cage. J. Chem. Phys. 2013;138:094312-1–094312-7. doi:10.1063/1.4793707.

[61] Kwapien K, Sierka M, Döbler J, et al. Structural diversity and flexibility of MgO gas-phase clusters. Angew. Chem. 2011;50:1716–1719. doi:10.1002/anie.201004617.

[62] Bhattacharya S, Sonin BH, Jumonville CJ, et al. Computational design of nanoclusters by property-based genetic algorithms: tuning the electronic properties of $(TiO_2)_n$ clusters. Phys. Lett. B. 2015;91:241115-1–241115-5. doi:10.1103/PhysRevB.91.241115.

[63] Burow AM, Wende T, Sierka M, et al. Structures and vibrational spectroscopy of partially reduced gas-phase cerium oxide clusters. Phys. Chem. Chem. Phys. 2011;13:19393–19400. doi:10.1039/C1CP22129A.

[64] Ding X-L, Li Z-Y, Meng J-H, et al. Density-functional global optimization of $(La_2O_3)_n$ clusters. J. Chem. Phys. 2012;137:214311-1–214311-7. doi:10.1063/1.4769282.

[65] Alexandrova AN. $H\cdot(H_2O)_N$ clusters: microsolvation of the hydrogen atom via molecular *ab initio* gradient embedded genetic algorithm (GEGA). J. Phys. Chem. A. 2010;114:12591–12599. doi:10.1021/jp1092543.

[66] Kiran B, Kandalam AK, Xu J, et al. Al6H18: a baby crystal of γ-AlH3. J. Chem. Phys. 2012;137:134303-1–134303-5. doi:10.1063/1.4754506.

[67] Fernandez-Lima FA, Neto OPV, Pimentel AS, et al. Theoretical and experimental study of negative LiF clusters produced by fast ion impact on a polycrystalline LiF target. J. Phys. Chem. A. 2009;113:1813–1821. doi:10.1021/jp905138d.

[68] Wang LM, Huang W, Averkiev BB, et al. CB_7^-: experimental and theoretical evidence against hypercoordinate planar carbon. Angew. Chem. Int. Ed. 2007;46:4550–4553. doi:10.1002/anie.200700869.

[69] Huynh MT, Alexandrova AN. Persistent covalency and planarity in the $B_nAl_{6-n}^{2-}$ and $LiB_nAl_{6-n}^-$ (n = 0–6) cluster ions. J. Phys. Chem. Lett. 2011;2:2046–2051. doi:10.1021/jz200865u.

[70] Xiang H, Wei S-H, Gong X. Structures of $[Ag_7(SR)_4]$- and $[Ag_7(DMSA)_4]$. J. Am. Chem. Soc. 2010;132:7355–7360. doi:10.1021/ja9108374.

[71] Huang X, Sai L, Jiang X, et al. Ground state structures, electronic and optical properties of medium-sized Na_n^+ (n = 9, 15, 21, 26, 31, 36, 41, 50 and 59) clusters from *ab initio* genetic algorithm. Eur. Phys. J. D. 2013;67:43-1–7. doi:10.1140/epjd/e2013-30539-2.

[72] Liang X, Huang X, Su Y, et al. Structures and electronic properties of neutral and anionic Ca_n (n = 2–22) clusters. Chem. Phys. Lett. 2015;634:255–260. doi:10.1016/j.cplett.2015.05.064.

[73] Sai L, Zhao J, Huang X, et al. Structural evolution and electronic properties of medium-sized gallium clusters from *ab initio* genetic algorithm search. J. Nanosci. Nanotechnol. 2012;12:132–137. doi:10.1166/jnn.2012.5126.

[74] Hong L, Wang H, Cheng J, et al. Atomic structures and electronic properties of small Au–Ag binary clusters: effects of size and composition. J. Comp. Theo. Chem. 2012;993:36–44. doi:10.1016/j.comptc.2012.05.027.

[75] Huang X, Su Y, Sai L, et al. Low-energy structures of binary Pt–Sn clusters from global search using genetic algorithm and density functional theory. J. Cluster. Sci. 2015;26:389–409. doi:10.1007/s10876-014-0829-7.

[76] Huang X, Lu S-J, Liang X, et al. Structures and electronic properties of $V_3Si_n^-$ (n = 3–14) clusters: a combined *ab initio* and experimental study. J. Phys. Chem. C. 2015;119:10987–10994. doi:10.1021/jp5112845.

[77] Huang X, Zhao J, Su Y, et al. Design of three-shell icosahedral matryoshka clusters A@B12@A20 (A = Sn, Pb; B = Mg, Zn, Cd, Mn). Sci. Rep. 2014;4:6915–6915. doi:10.1038/srep06915.

[78] Sai L, Tang L, Huang X, et al. Lowest-energy structures of $(WO_3)_n$ ($2 \le n \le 12$) clusters from first-principles global search. Chem. Phys. Lett. 2012;544:7–12. doi:10.1016/j.cplett.2012.06.050.

[79] Alexandrova AN, Boldyrev AI. Search for the $Li_n^{0/+1/-1}$ (n = 5–7) lowest-energy structures using the *ab initio* gradient embedded genetic algorithm (GEGA). Elucidation of the chemical bonding in the lithium clusters. J. Chem. Theo. Comput. 2005; 1: 566–580. doi:10.1021/ct050093g.

[80] Oakley MT, Johnston RL, Wales DJ. Symmetrisation schemes for global optimisation of atomic clusters. Phys. Chem. Chem. Phys. 2013;15:3965–3976. doi:10.1039/C3CP44332A.

[81] Delley B. An all-electron numerical method for solving the local density functional for polyatomic molecules. J. Chem. Phys. 1990;92:508–517. doi:10.1063/1.458452.

[82] Delley B. From molecules to solids with the DMol^3 approach. J. Chem. Phys. 2000;113:7756–7764. doi:10.1063/1.1316015.

[83] Kresse G, Furthmüller J. Efficient iterative schemes for *ab initio* total-energy calculations using a plane-wave basis set. Phys. Rev. B. 1996;54:11169–11186. doi:10.1103/PhysRevB.54.11169.

[84] Aprà E, Ferrando R, Fortunelli A. Density-functional global optimization of gold nanoclusters. Phys. Rev. B. 2006;73:205414. doi:10.1103/PhysRevB.73.205414.

[85] Li J, Li X, Zhai H-J, et al. Au_{20}: a tetrahedral cluster. Science. 2003;299:864–867. doi:10.1126/science.1079879.

[86] Wales DJ, Doye JPK. Global optimization by basin-hopping and the lowest energy structures of Lennard-Jones clusters containing up to 110 atoms. J. Phys. Chem. A. 1997;101:5111–5116. doi:10.1021/jp970984n.

[87] Kroto HW, Heath JR, O'brien SC, et al. C_{60}: buckminsterfullerene. Nature. 1985;318:162–163.

[88] Gonzalez Szwacki N, Sadrzadeh A, Yakobson BI. B_{80} fullerene: an *ab initio* prediction of geometry, stability, and electronic structure. Phys. Rev. Lett. 2007;98:166804-1–166804-4. doi:10.1103/PhysRevLett.98.166804.

[89] Li W-L, Chen Q, Tian W-J, et al. The B_{35} cluster with a double-hexagonal vacancy: a new and more flexible structural motif for borophene. J. Am. Chem. Soc. 2014;136:12257–12260. doi:10.1021/ja507235s.

[90] Piazza ZA, Hu H-S, Li W-L, et al. Planar hexagonal B36 as a potential basis for extended single-atom layer boron sheets. Nat. Commun. 2014;5: 205411-1–205411-5. doi:10.1038/ncomms4113.

[91] Zhai HJ, Zhao YF, Li WL, et al. Observation of an all-boron fullerene. Nat. Chem. 2014;6:727–731. doi:10.1038/nchem.1999.

[92] Shang C, Liu Z-P. Stochastic surface walking method for structure prediction and pathway searching. J. Chem. Theo. Comput. 2013;9:1838–1845. doi:10.1021/ct301010b.

[93] Kiran B, Bulusu S, Zhai H-J, et al. Planar-to-tubular structural transition in boron clusters: B_{20} as the embryo of single-walled boron nanotubes. Proc. Natl. Acad. Sci. USA. 2005;102:961–964. doi:10.1073/pnas.0408132102.

[94] Lin SS. Detection of large water clusters by a low rf quadrupole mass filter. Rev. Sci. Instrum. 1973;44:516–517. doi:10.1063/1.1686172.

[95] Hodges MP, Wales DJ. Global minima of protonated water clusters. Chem. Phys. Lett. 2000;324:279–288. doi:10.1016/S0009-2614(00)00584-4.

[96] Wu C-C, Lin C-K, Chang H-C, et al. Protonated clathrate cages enclosing neutral water molecules: $H^+(H_2O)_{21}$ and $H^+(H_2O)_{28}$. J. Chem. Phys. 2005;122:074315–074315. doi:10.1063/1.1843816.

[97] Zwier TS. The structure of protonated water clusters. Science. 2004;304:1119–1120. doi:10.1126/science.1098129.

[98] Kozack RE, Jordan PC. Structure of $H^+(H_2O)_n$ clusters near the magic number n = 21. J. Chem. Phys. 1993;99:2978–2984. doi:10.1063/1.465204.

[99] Bauernschmitt R, Ahlrichs R. Treatment of electronic excitations within the adiabatic approximation of time dependent density functional theory. Chem. Phys. Lett. 1996;256:454–464. doi:10.1016/0009-2614(96)00440-X.

[100] Noya EG, Doye JPK, Wales DJ, et al. Geometric magic numbers of sodium clusters: interpretation of the melting behaviour. Eur. Phys. J. D. 2007;43:57–60. doi:10.1140/epjd/e2007-00092-x.

[101] Aguado A, Kostko O. First-principles determination of the structure of Na_N and Na_N^- clusters with up to 80 atoms. J. Chem. Phys. 2011;134:164304-1–164304-12. doi:10.1063/1.3582911.

[102] Zheng W. Negative ion photoelectron spectroscopy of metal clusters, metal-organic clusters, metal oxides, and metal-doped silicon clusters. PhD Thesis (K. Bowen, Advisor). Baltimore, MD: Johns Hopkins University; 2005.

[103] Huang X, Xu H-G, Lu S, et al. Discovery of a silicon-based ferrimagnetic wheel structure in $V_xSi_{12}^-$ (x = 1-3) clusters: photoelectron spectroscopy and density functional theory investigation. Nanoscale. 2014;6:14617–14621. doi:10.1039/C4NR03130J.